

## Equilibrium reconstruction in the presence of 3D external magnetic perturbations on ASDEX Upgrade

J. C. Fuchs<sup>1</sup>, M. Dunne<sup>2</sup>, R. Fischer<sup>1</sup>, L. Giannone<sup>1</sup>, A. Herrmann<sup>1</sup>, B. Kurzan<sup>1</sup>, P. de Marné<sup>1</sup>,  
P. J. McCarthy<sup>2</sup>, E. Strumberger<sup>1</sup>, W. Suttrop<sup>1</sup>, W. Schneider<sup>1</sup>, E. Wolfrum<sup>1</sup>,  
and the ASDEX Upgrade Team<sup>1</sup>

<sup>1</sup>Max-Planck-Institut für Plasmaphysik, EURATOM Association, Garching, Germany

<sup>2</sup>Department of Physics, University College Cork, Ireland.

### Introduction

At ASDEX Upgrade the set of non-axisymmetric magnetic perturbation coils (MP coils) has recently been extended and now consists of each eight coils both above and below the midplane, which allow magnetic perturbations with toroidal mode numbers up to  $n = 4$ , with varying relative phase between the upper and lower rings and varying toroidal orientation. The MP coils have successfully been used to mitigate the plasma energy loss and peak divertor power load linked to Edge Localized Modes (ELMs), whereas concerning confinement, plasma density and impurity concentration both unperturbed ELMy reference discharges and plasmas with mitigated ELMs show a similar behavior [1,2].

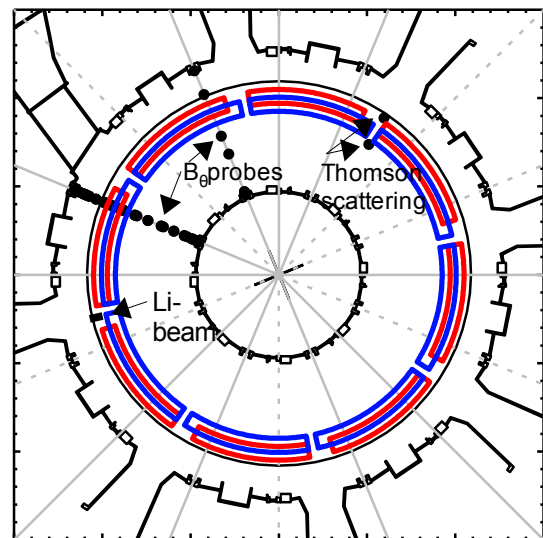


Figure 1: Toroidal view of ASDEX Upgrade with the position of the upper (red) and lower (blue) perturbation coils and of some diagnostics used in this paper: magnetic probes at two toroidal positions, Thomson scattering (edge and core) and lithium beam

### Measurements of the toroidal variation of the magnetic field

The main tool for equilibrium reconstruction at ASDEX Upgrade is the CLISTE interpretative code [3] which numerically solves the Grad-Shafranov equation as a best fit to a set of experimental measurements, especially from magnetic probes and flux loops. Since the Grad-Shafranov equation assumes toroidal symmetry of the plasma, any effects of the non-axisymmetric magnetic perturbations of the new saddle coils on the equilibrium is not taken into account. The magnetic probes in ASDEX Upgrade which measure the poloidal component of the magnetic field are all located at one toroidal position, where a dense set of 40 probes around the torus inside the vessel and 32 probes outside the vessel are available. In order to get an estimation of the toroidal variation of the magnetic field and the equilibrium induced by the perturbation coils another set of magnetic probes toroidally separated by  $45^\circ$  from the original probes has recently been activated (figure 1). Unfortunately it was not

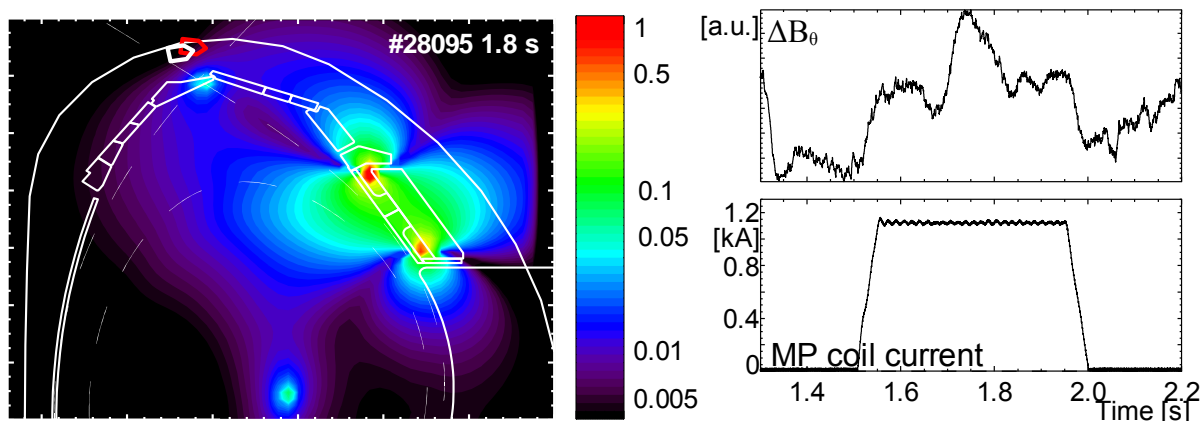


Figure 2: The left picture shows a poloidal cross section through the upper half of ASDEX Upgrade, where the colors (from a logarithmic color scale) indicate the relative difference of the poloidal magnetic field due to the perturbation coils between two positions toroidally separated by  $45^\circ$  as a fraction to the plasma induced poloidal magnetic field  $|(B_{\theta,MP}(\varphi=157.5^\circ)-B_{\theta,MP}(\varphi=112.5^\circ))/B_{\theta,Plasma}|$ . The dashed lines show the separatrix and the flux surface through the 2<sup>nd</sup> (upper) X-point. The two arrows (red and white) near the top of the vessel denote the position and direction of two  $B_\theta$  probes which are also toroidally separated by  $45^\circ$ . The time evolution of the difference of the measurements from these two probes during a phase where the perturbation coils are switched on and off is shown in the upper part of the right picture, the corresponding coil current is shown in the lower part.

possible to install these new probes at exactly the same poloidal positions as the old probes, and only 7 of them are already in operation.

Figure 2 shows for a discharge where the perturbation coils have been used in  $n=2$  configuration the relative difference of the poloidal magnetic field due to the perturbation coils between the toroidal positions of the old and new magnetic probes as a fraction to the plasma induced poloidal magnetic field  $|(B_{\theta,MP}(\varphi=157.5^\circ)-B_{\theta,MP}(\varphi=112.5^\circ))/B_{\theta,Plasma}|$  (note the logarithmic color scale). (For probes toroidally separated by  $45^\circ$  the largest differences would be found for  $n=4$  configurations of the perturbation coils, but since the commissioning of the new probes no such discharges have been performed.) As expected the main influence of the perturbation coils on the poloidal magnetic field is found in the direct vicinity of the coils, but also around the magnetic axis and the two X points where the poloidal field of the plasma vanishes. In all other parts however the influence of the perturbation coils on the poloidal field is negligible. Therefore up to now there remains only one pair of magnetic probes near the secondary (upper) X point where one can expect to see the influence of the perturbation coils on the difference of the poloidal field measured by these probes, as shown in the right part of figure 2. This measured difference of only a few percent is also consistent with the previously measured mutual inductance of the saddle coils and the magnetic probes [4], and due to the fact that the two probes are not exactly at the same poloidal position and even have a slightly different poloidal direction the influence of the perturbation coils on their measurements is often overlaid with other effects like small changes in the plasma position.

### Three-dimensional equilibrium reconstruction

Due to their limitations in number and position these new magnetic probes are not sufficient

to reconstruct the full three-dimensional equilibrium with a sufficient accuracy. Therefore, other methods have been used to get an estimation of the toroidal variation of the equilibrium: An easy way is to start from an unperturbed, toroidal symmetric equilibrium and to add the vacuum field of the perturbation coils. Using a three-dimensional field line tracing code it could be shown for  $n=2$  perturbations [3] that the separatrix is perturbed by the saddle coils sinusoidally around the torus compared to the unperturbed equilibrium, the same behavior is now also found for  $n=4$  perturbations. Also a shift of plasma profiles around the separatrix was found to be consistent with this perturbation of the separatrix [4].

However, the vacuum field approach does not take into account any shielding currents by the plasma on the perturbation field. It allows that the field lines can penetrate arbitrarily into the plasma which leads to a dissolution of the flux surfaces and a formation of a 'stochastic' region with islands, whose depth depends on the configuration of the perturbation coils. However, up to now no experimental evidence in edge profiles could be found for a stochastic region or island formation [5].

The opposite approach is done by calculating the three-dimensional equilibrium using the NEMEC code which was originally developed for stellarator geometry. This code is the free-boundary version of the VMEC code which calculates ideal MHD equilibria by minimizing the total plasma energy  $W_P$  in a toroidal domain [6]. Since it assumes nested flux surfaces inside the plasma it does not permit any formation of a stochastic layer.

It is found that the form of the separatrix in equilibria calculated by NEMEC is consistent with the deformation of the separatrix due to the magnetic perturbations calculated with the vacuum field approach. Furthermore, NEMEC calculated equilibria can also show the toroidal variation of the interior flux surfaces, which can not be done with the vacuum field approach. This can help when trying to map measurements from different toroidal positions onto a common flux surface coordinate, assuming constant values on flux surfaces: Figure 3 shows electron density profiles measured by the Li-beam and Thomson-scattering diagnostics, which are toroidally separated by  $137^\circ$  (figure 1), for an H-mode discharge with phases without MP

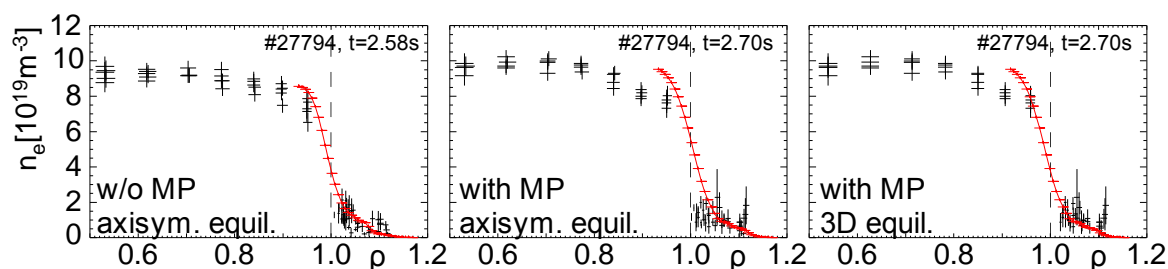


Figure 3: Density profiles from the Li-beam (red) and Thomson-scattering (black) diagnostics mapped on the flux surface coordinate  $\rho_{pol}$  for time points shortly before the perturbation coils are switched on (left) and shortly after the current of the perturbation coils is ramped up (middle and right). In the middle graph an unperturbed, axisymmetric equilibrium has been used for mapping the measurements to  $\rho_{pol}$ , whereas in the right graph a full three-dimensional equilibrium calculated with the NEMEC code has been used.

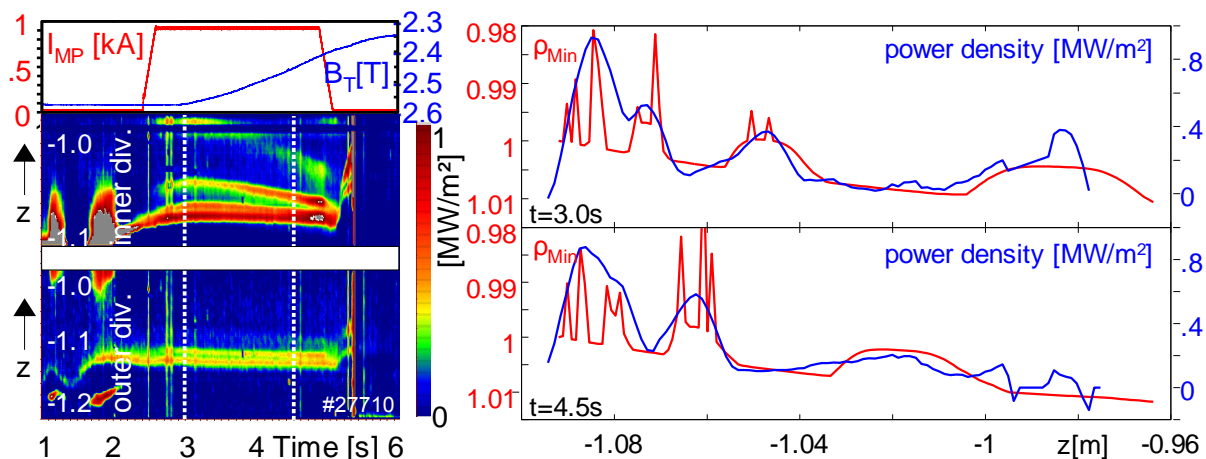


Figure 4: Left picture: Power density measured by thermographic cameras along the outer and inner divertor plates as a function of time during a discharge with MP coils and a  $B_T$ -ramp. Right picture: Power density along the inner divertor plate at the two indicated time points (blue) and minimal  $\rho_{pol}$  (red) for field lines starting at this target plate.

(left graph) and upper MP coils in  $n=2$  configuration (middle and right graph). Whereas without perturbations the mapping between these two diagnostics is quite good, it becomes worse when the MP coils are applied, if one uses the unperturbed, axisymmetric equilibrium. If instead the NEMEC calculated equilibrium is used, the mapping becomes better again. Since NEMEC calculates flux surfaces only inside the plasma, measurements outside the separatrix have been mapped by applying the width of the deformation of the last closed flux surface at the height and toroidal position of the respective measurement.

### Strike line splitting

In phases where the magnetic perturbation coils are used, often, but not always, several maxima of the power density are recorded by thermographic cameras in the vicinity of the calculated strike point both on the inner and the outer target plate in the divertor (figure 4, left picture), called 'strike line splitting'. The position of these maxima can be explained with the help of the simple vacuum field approach: When following field lines starting at the divertor plates observed by the thermographic cameras, one finds a correlation between the measured power density and the depth  $\rho_{Min}$  how far these field lines penetrate into the plasma (figure 4, right picture), which leads to an effective parallel transport of hot, dense plasma onto the divertor [7,8]. Fine structures in the  $\rho_{Min}$  distribution from the field lines origin from the stochastic layer inside the plasma and are smoothed out in the measured power distribution, probably due to transport perpendicular to the field lines. However, although this model may describe the positions of these strike points, it cannot explain under which conditions strike point splitting occurs.

### References

- [1] W. Suttrop et al., PPCF **53** (2011), 124014
- [2] W. Suttrop et al., this conference, P2.092
- [3] P.J. McCarthy et al., PPCF **54** (2012), 015010
- [4] J. C. Fuchs et al., ECA **35G** (2011), P1.090
- [5] R. Fischer et al., submitted to PPCF
- [6] S.P. Hirshman, Comput. Phys. Com. **43** (1986) 143
- [7] T. Lunt et al., Nuclear Fusion **52** (2012), 054013
- [8] H. W. Müller et al., submitted to J Nucl Materials